JMEPEG (2004) 13:309–315
DOI: 10.1361/10599490419289

1059-9495/$19.00

# High-Temperature Electrical Testing of a Solid Oxide Fuel Cell Cathode Contact Material

*K. Scott Weil*

*(Submitted 5 January 2004)*

**The development of high-temperature solid-state devices for energy generation and environmental control applications has advanced remarkably over the past decade. However, there remain a number of technical barriers that still impede widespread commercial application. One of these, for example, is the development of a robust method of conductively joining the mixed-conducting oxide electrodes that lie at the heart of the device to the heat resistant metal interconnect used to transmit power to or from the electrodes and electrochemically active membrane. This study investigated the high-temperature electrical and microstructural characteristics of a series of conductive glass composite paste junctions between two contact materials representative of those used in solid-state electrochemical devices, lanthanum calcium manganate, and 430 stainless steel.**

**Keywords** electrical contact, interconnect, mixed ionic/electronic conductor, solid oxide fuel cell

## 1. Introduction

Mixed ionic/electronic conducting (MIEC) oxides, such as $SrFeCo_{0.5}O_x$, $(La_{0.6}Sr_{0.4})(Co_{0.2}Fe_{0.8})O_3$, and $BaCeO_3$, are a class of ceramics that contain ionic and electronic carriers in high enough concentration that both forms of charge conduction are exhibited at a high level, typically at temperatures in excess of 500 °C. Due to their properties, the demand for MIEC oxide-based devices has grown considerably. The value of the present-day market is conservatively estimated to be $3 billion, with particularly high growth rates in automotive systems, environmental control, and energy generation technology where the devices are used primarily as amperometric chemical sensors.[1] Solid oxide fuel cells (SOFCs) represent an even larger potential market than that established for chemical sensors. These electrochemical devices convert the chemical energy from fossil fuels into electricity in a highly efficient manner and may find application in a number of energy generation applications, from auxillary power units used in automobiles and trucks to megawatt generators used as part of the electric power grid. MIEC oxides are used in SOFCs as electrodes, carrying out charge separation and charge transfer at the electrolyte/electrode interface, and as agents to increase the electrocatalytic activity of the electrodes with respect to fuel reformation.[2] If the ionic conductivity of a given MIEC oxide is high enough, it can be used as an electrically driven oxygen-ion transport membrane for oxygen gas separation, partial hydrocarbon oxidation, and waste reduction and recovery.[3] MIEC oxide-based membrane technology offers the potential to separate oxygen from air with far greater efficiency and at one-third lower cost than the cryogenic processing technology used today. And unlike cryo-separation, oxygen transport membranes operate at high temperatures, making them ideally suited for direct integration with coal gasification plants.[4]

Underlying the excitement over the potential value of MIEC oxides is the engineering challenge of how to effectively incorporate these materials into practical devices. Opportunities to fully exploit the unique properties of these advanced ceramics depend in large part on our ability to develop reliable joining techniques. However, because MIEC-based device technology is essentially restricted to high-temperature operation, only a limited number of joining technologies are applicable. Further complicating the joining process is the need for the ceramic-to-metal joint to be electrically conductive so that current can either be drawn from the MIEC oxide, in the case of SOFC applications, or be carried to the MIEC oxide to initiate ionic conduction, as is required in oxygen separation and electrocatalytic devices.

An example of where MIEC oxide/metal joining is used in SOFCs is shown in Fig. 1(a), which displays a schematic drawing of a typical planar stack design. A cut-away view depicting the joining arrangement between the metal interconnect and the MIEC oxide cathode is seen in Fig. 1(b). The conditions under which the fuel cell, and therefore the MIEC oxide/metal joint, is typically run are noted. To generate a sufficient rate of ionic/electronic transport within a solid-state fuel cell, it must be operated at high temperature, normally on the order of 500-1000 °C. The present analysis assumes an operating temperature of 750 °C, which is sufficient for both SOFC and oxygen generation applications.[5,6] Unfortunately, this temperature is also high enough for thermally activated processes to take place that may be deleterious to device performance, such as

This paper was presented at the Fuel Cells: Materials, Processing, and Manufacturing Technologies Symposium sponsored by the Energy/Utilities Industrial Sector & Ground Transportation Industrial Sector and the Specialty Materials Critical Technologies Sector at the ASM International Materials Solutions Conference, October 13-15, 2003, in Pittsburgh, PA. The symposium was organized by P. Singh, Pacific Northwest National Laboratory, S.C. Deevi, Philip Morris USA, T. Armstrong, Oak Ridge National Laboratory, and T. Dubois, U.S. Army CECOM.

**K. Scott Weil,** Energy Science and Technology Division, Pacific Northwest National Laboratory, Richland, WA 99352. Contact e-mail: scott.weil@pnl.gov.

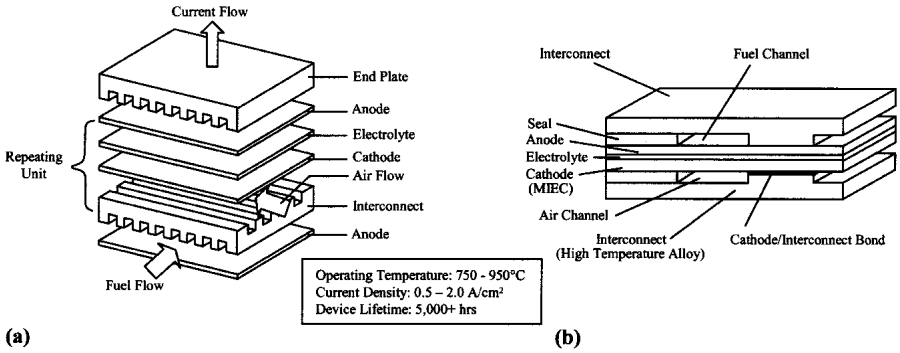


**Fig. 1 (a)** A schematic drawing of a planar solid oxide fuel cell (SOFC) stack design. **(b)** A cut-away view of the typical joining arrangement between the metal interconnect and mixed conducting cathode component.

interdiffusion, oxidation, and interfacial solid-state reaction; particularly over the expected lifetimes of these devices, estimated to be 3000-30,000+ h depending on the specific application. Thus, the joint must be capable of resisting structural degradation at these conditions, while conducting high electrical current with minimal $I^2R$ loss to maximize device performance. Typical current densities range from 0.5 to 2.0 A/cm$^2$.

A key issue with respect to electrical conduction is the mobility of oxygen in the MIEC oxide and the effect this may have on scale formation within the ceramic-to-metal bond region. A second concern is the effect that high current density may have on the rate of diffusion and chemical reaction at the ceramic/metal interface. Formation of a continuous, nonconductive scale or reaction product at this interface will impede transverse current flow and must be avoided. Depending on the application, other functional requirements may include: (a) hermeticity over the lifetime of the device, (b) the ability to survive thermal cycling from operating temperature to room temperature, and/or (c) low raw material and manufacturing costs.

The use of noble metal pastes and metallization layers, in particular platinum (Pt), is popular in joining small MIEC oxide samples to metal interconnects for research and development work and for testing purposes. However, employing Pt and other noble metals, outside of silver (Ag) perhaps, for the manufacture of commercial devices is cost prohibitive. Noble metal interlayers also display at best only weak mechanical bonding with MIEC oxides; thus, joints constructed with these materials will exhibit poor bond strengths. In addition, it has been reported in the case of Pt that the metal migrates during device operation, causing electrochemical performance to degrade after several hundred hours of use.[7] A composite joining system may offer the best means of developing a high performance MIEC oxide/metal interconnect bond. One concept is to use a conductive glass-composite wherein an electrically conductive phase, such as Ag or tin oxide, is dispersed in a high temperature glass or glass-ceramic matrix. In many ways, this material system is analogous to the conductive frits that have been used for a number of years in the microelectronics industry as thick film resistors,[8] with the exception that the new composite must be functional at much higher temperature. A contact paste formulated in this manner can be heat treated directly in air and should be highly conductive during operation assuming that the conductive phase is randomly dispersed in the composite at a volume fraction greater than the percolation limit, i.e., it is continuously interconnected from one side of the joint to the other. The greatest concern with this concept is whether a resistive reaction zone will form between the contact material and either of the conductive faying surfaces. The study described here considers three potential conductive glass composite systems, each employing a high-temperature barium aluminosilicate glass as the matrix and one of the following as the dispersed conductive phase: tin-doped indium oxide, lanthanum calcium chromate, or Ag. Long-term, high-temperature conductivity testing was conducted on the most promising of the three and selected joint samples were subsequently examined microstructurally via scanning electron microscopy (SEM).

## 2. Experimental

### 2.1 Materials

Lantanum calcium manganate (LCM), $(La_{0.8}Ca_{0.2})MnO_3$, and 430 stainless steel (430SS) were used, respectively, as the model cathode/interconnect system to carry out the initial development and testing effort on conductive glass-composite joining. LCM was selected because: (a) it is a candidate electrode material for a variety of high-temperature solid-state devices,[9-11] (b) it has a coefficient of thermal expansion (CTE) that matches those of a number of candidate interconnect materials over the application temperature range, and (c) it typically displays better thermal stability and chemical compatibility with adjacent oxide materials, including glasses, than a number of related perovskite compounds. The LCM samples were fabricated by tape casting. LCM powder (Praxair Specialty Ceramics, Inc., Woodinville, WA) was ball milled for 1½ days with polyvinylbenzene in a methyethyl ketone/isopropyl alcohol solvent using PS-21A (Witco, Inc., Petrolia, PA) as a dispersant. The slurry was cast onto silicone coated mylar, forming a ~0.16 mm thick tape when dry. The tapes were cut into ~1.4 cm squares and the squares were paired and run through heated rolls to form laminated pieces. These were then sintered in air at 1300 °C for two hours, yielding ~1.1 cm square samples measuring nominally 250 μm in thickness with densities in excess of 89% of theoretical.

The 430 stainless steel was chosen as the interconnect ma-

terial because: (a) its CTE closely matches that of LCM, (b) it displays good oxidation properties at high temperature, (c) it forms a continuous chromia scale, which when thin enough will be sufficiently conductive at 750 °C, and (d) it is the most widely produced ferritic stainless sheet product, making it a strong low-cost candidate for commercial high temperature electrochemical devices. As-received ~½ mm (20 mil) thick 430SS sheet was sheared into 2 × 2 cm square samples and polished on both sides with 1200 grit SiC paper. The samples were flushed with deionized water to remove the grit and ultrasonically cleaned in acetone for 10 min.

A barium aluminosilicate based glass was used as the matrix in the composite joining material. The glass, referred to as G-18, was developed in-house at Pacific Northwest National Laboratory for use as a high-temperature sealing glass[12] and was produced as powder (average particle size of 34 μm) in large-scale batches by the Viox Corporation (Seattle, WA). The glass is fomulated by melting and homogenizing the following mixture of oxides (by weight percent): 56.4% BaO, 22.1% $SiO_2$, 5.4% $Al_2O_3$, 8.8% CaO, and 7.3% $B_2O_3$. In its vitreous state, the average CTE of G-18 from room temperature to 600 °C is $11.8 \times 10^{-6}$ m/K, closely matching that of LCM and 430. When devitrified, after ~120 h at 750 °C, the CTE drops to $\sim 10.0 \times 10^{-6}$ m/K.[13]. In a series of small coupon experiments, G-18 displayed excellent wetting and joining characteristics with several ferritic stainless steels, including 430, 446, Ebrite and 29-4. The glass powder can be used by casting it into 100 μm thick tapes using an appropriate tape casting procedure or by suspending the powder in a viscous organic binder to form a paste. Both fabrication techniques were used in this study as described below.

Three electrically conductive materials expected to be chemically compatible with the glass matrix were examined in an initial set of scoping experiments: tin-doped indium oxide (ITO – with an $In_2O_3$ to $SnO_2$ ratio of 90:10 wt.%; 38 μm average particle diameter; Alfa Aesar, Ward Hill, MA), $(La_{0.8}Ca_{0.2})CrO_3$ (LCC;1 μm average particle diameter; Praxair SC Inc.), and Ag (5.5 μm average particle diameter; Alfa Aesar). Using these, six different pastes were formulated. Each paste contained one type of conductive powder in either a 35 or 65 vol% concentration with the glass matrix. The pastes were prepared by dry mixing the appropriate amounts of conductive material and glass powder; adding a binder, BX-18 (Ferro Corporation, Cleveland, OH); and thoroughly mixing the blend on a three-roll mill. All formulations were found to have acceptable thixotropic properties for the wetting and joining experiments. Tape cast formulations were prepared by mill mixing the appropriate quantities of glass and conductive powders with polyvinyl benzene in a mixture of the methylethyl ketone/isopropyl alcohol solvent and the PS-21A dispersant, casting the slurry onto silicone coated mylar, and allowing to air dry. The tapes were cast at a thickness of ~0.12 mm, forming a ~100 μm thick sheet when dry.

### 2.2 Testing and Characterization

Wetting experiments were conducted in a static air box furnace. The composite pastes were spread on cleaned samples of LCM and 430SS, heated at 5 °C/min to 850 °C, and held at temperature for 1 h. The samples were then cooled at 5 °C/min to 750 °C and held isothermally for an additional 4 h, after which they were allowed to cool to room temperature at 5 °C/min. The wetting angle and degree of coverage of the glass composite over the substrate, as well as the electrical resistance of the sample from the back side of the substrate to the top surface of the glass composite were measured at room temperature.

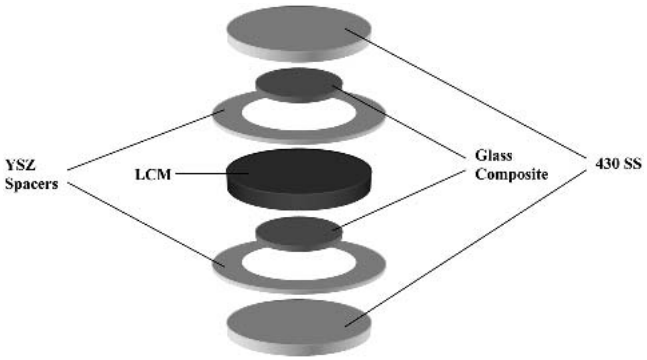


**Fig. 2** Schematic illustration of the double-joint samples used in conductivity testing.

The wetting angle was averaged from a set of eight separate measurements, taken after mounting the sample on a square block and photographing it side-on under 50× magnification. The sample was examined on all 4 sides recording two measurements per side, one from each viewable air/glass-composite/substrate interface. The degree of glass-composite coverage over the substrate was noted in a qualitative manner by simply observing whether the composite paste tended to spread over or shrink away from the substrate in a uniform manner, or instead left behind partially covered patches of substrate as the glass matrix sintered and eventually melted. The electrical measurements made during the initial screening study were conducted at room temperature using a simple two-probe technique. Pt electrodes measuring ~½ cm in diameter were joined with Pt paste to the top and bottom surfaces of the wetting samples. In the case of the metal substrates, the oxide scale on the outer surface was removed with 1200 grit paper prior to electrode attachment. To cure the Pt contact paste, the samples were heated in a vacuum oven to 150 °C and held isothermally for 2 h. Once bonded, each lead was connected in series with a HP 3263A direct current (dc) power supply and a HP 34401A multimeter (Hewlett Packard Corp., Palo Alto, CA). Current measurements were recorded for 0.01, 0.1, 1, and 10 V of potential applied across the sample.

Long-term, high-temperature electrical testing was conducted on contact samples using a modified four-point probe technique. As shown in Fig. 2, the samples were prepared as double joints to facilitate good connection of the leads and to provide an accurate measure of the average electrical resistance of the conducting joint. The two substrates were fabricated in a circular geometry (2.5 cm diameter) and the 100 μm thick, tape cast glass composite was laser cut into circles measuring 1.5 cm in diameter. Also shown in Fig. 2 are yttria-stabilized zirconia (YSZ) spacers measuring 3 cm outer diameter × 2 cm inner diameter × 50 μm thick that were used as internal stops within the sample to set the thickness of the glass composite

**Table 1 Properties of Six Glass-Composite Contact Materials**

| | Composition | | Estimated Wetting Angle | | Degree of Spreading | | Electrical Resistance | |
|---|---|---|---|---|---|---|---|---|
| Sample | vol% Glass | vol% 2nd Phase | LCM | 430 | LCM | 430 | LCM (a) | 430 |
| ITOG-35 | 65 | 35-ITO | 21° | Sample Detached | Uniform | Sample Detached | 72 Ω | Sample Detached |
| ITOG-65 | 35 | 65-ITO | 29° | Sample Detached | Non-Uniform | Sample Detached | 48 Ω | Sample Detached |
| LCCG-35 | 65 | 35-LCC | 32° | 35° | Uniform | Uniform | 141 Ω | 127 Ω |
| LCCG-65 | 35 | 65-LCC | 28° | 46° | Non-Uniform | Uniform | 122 Ω | 96 Ω |
| AgG-35 | 65 | 35-Ag | 29° | 37° | Uniform | Uniform | 27 Ω | <0.1 Ω |
| AgG-65 | 35 | 65-Ag | 24° | 42° | Uniform | Uniform | 26 Ω | <0.1 Ω |

(a) Note: The baseline through-thickness resistance of the LCM substrate measured between 24 and 28 Ω.

layers. Prior to sample assembly, two Pt leads were spot welded to the back of each metal substrate. The samples were then assembled (with each layer centered), placed under a 200 g dead load, and heat treated in air using the same schedule used in the wetting experiments described above. Once joined, one lead each from the top and bottom of the sample was connected to a HP 3263A dc power supply and the other two were connected to a HP 34401A multimeter and datalogger forming a parallel circuit. The sample was placed into an alumina tube furnace and heated at 10 °C/min to 750 °C and held isothermally under 20 $cm^3$/min of flowing air for the duration of the test. Voltage measurements were recorded every five seconds as 1.5 A of dc current was continuously applied to the sample during testing. Subsequent microstructural analysis of the joints was conducted on polished cross-sectioned samples using a JEOL JSM-5900LV (JOEL Corp., Peabody, MA) scanning electron microscope (SEM) equipped with an Oxford energy dispersive x-ray analysis (EDX) system. To avoid electrical charging of the samples, they were carbon coated and grounded prior to analysis. Elemental profiles were determined across the joint interfaces in the line-scan mode.

## 3. Results and Discussion

### 3.1 Scoping Studies

Reported in Table 1 are the results from our initial screening experiments conducted to determine the composite joining system most suitable for further development and testing; that is, the system that demonstrated both acceptable wetting on each substrate and exhibited the lowest level of electrical resistance through the composite-to-substrate bond. Although the ITO-glass pastes displayed good spreading on both substrates, acceptable adhesion was found only in the LCM wetting samples. The LCC-based wetting samples displayed acceptable wetting and adhesion properties on both substrates, but exhibited fairly high levels of electrical resistance at room temperature; much higher than anticipated based on a simple rule-of-mixtures calculation. Although these values are expected to drop significantly at higher temperatures due to the inverse temperature dependence of LCC's resistivity, it is suspected that some chemical interaction took place between the LCC and the glass matrix that may have altered the bulk resistivity of the composite. Consequently, this system was set aside for further study at a future time. The most promising results were obtained using the Ag-glass composites, which compelled us to examine this system in more detail.

To determine the lowest Ag content at which the bond still exhibits an acceptably low vlaue of through-thickness resistance, electrical tests were conducted on a more extensive series of Ag-glass composite half joints. Using the technique described previously, four additional Ag-glass pastes were prepared that contained 15, 20, 25, and 30 vol% Ag in the high temperature glass matrix. Each paste was spread on both a LCM and a 430 substrate, heat treated as before, and examined. All six joining compounds displayed uniform spreading and low wetting angles on both substrates, ranging from 25° to 35° on LCM and 33° to 46° on 430. The glass-composite side of each half-joint sample was then ground flat, down to a thickness of 0.30 ± 0.03 mm for the composite. Pt leads were Ag pasted onto the top of the composite and either Ag pasted or spot welded to the backside of the LCM or 430 substrate, respectively. Four-point resistance testing was conducted at room temperature by measuring the voltage drop across the through-thickness direction of each sample under 250 mA of dc current.

Shown in Fig. 3 are the results from these tests. The measurements obtained on the LCM substrate show only a very slight decrease in through-thickness resistance with increasing Ag content in the composite. This can be attributed to the relatively high resistivity of the substrate at room temperature. At higher temperature, LCM becomes more conductive by several orders of magnitude and the resistance through these samples is expected to drop commensurately. Results from the glass-composite/430 half-joints display a nearly linear decrease in the through-thickness resistance as the Ag content in the composite increases from 20 to 65 vol%. The trend is similar to that predicted by Springett's theoretical percolation model, which describes the variation in conductivity with composition for a metal particle-insulator system.[14] Of course, it should be noted that the results in Fig. 3 account not only for the resistance through the composite, but also through the composite/metal interface and bulk metal. It is also apparent from Fig. 3 that regardless of the substrate, the 15 vol% Ag-glass composite is non-conductive, suggesting a threshold value of 15–20 vol% Ag is required for electrical conductivity in this system. This critical volume fraction of Ag also agrees quite well with Springett's model, which predicts a value of $V_c \sim 0.16 \pm 0.02$.[14]

With a Ag composition approximately halfway between the previously tested extremes, the 35 vol% Ag-glass composite was chosen as a convenient starting point for long-term testing. Plotted in Fig. 4 are area specific resistance (ASR) measure-

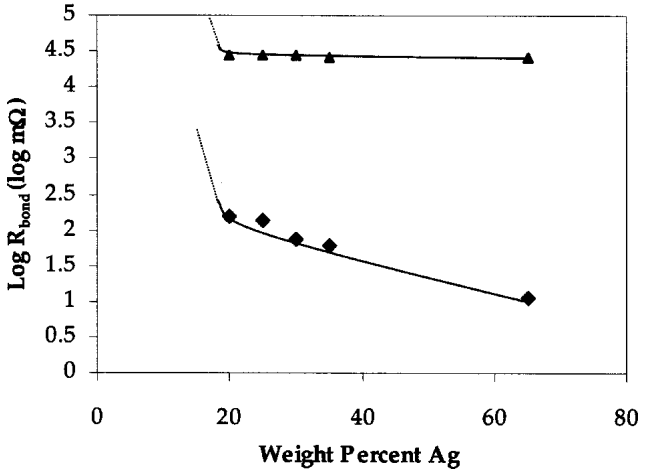


**Fig. 3** The through-thickness resistance of the Ag-glass composite as a function of Ag content, as measured on 430 stainless steel (♦) and LCM (▲) substrates at room temperature.

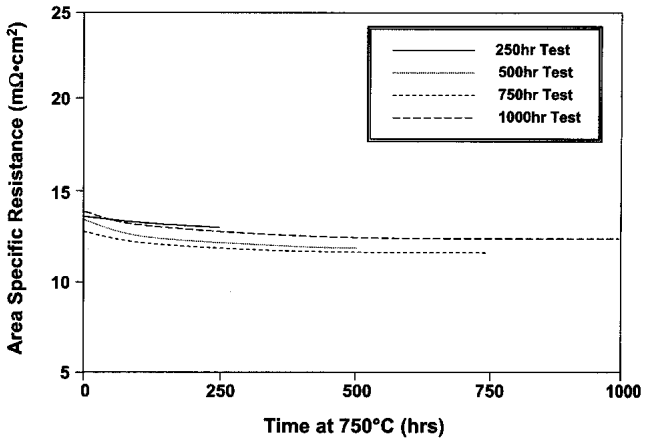


**Fig. 4** The area specific resistance of a series of double joint specimens as a function of time at 750 °C under 1.5 A dc current and 20 $cm^3$/min flowing dry air

ments of a series of double joint conductivity samples (430SS/Ag-glass/LCM/Ag-glass/430SS) as a function of time at 750 °C, under 1.5 A of dc current and 20 $cm^3$/min of flowing dry air. The samples were held at these conditions for 250, 500, 750, and 1000 h. The ASR calculations were made using the maximum cross-sectional area of the contact material, i.e., 3.14 $cm^2$, assuming full constraint of the glass composite by the two internal spacers within the conductivity sample. Note that none of the joint samples displays any degradation in electrical conductance with time. Instead each shows a slight improvement. As will be seen in the metallographic results, one possible reason for this is the interaction of Ag at the 430/glass-composite interface.

Shown in Fig. 5(a) is a cross-sectional micrograph of one of the 430/35 vol% Ag-glass/LCM joints in an as-formed conductivity sample. It is readily apparent that the Ag (visible as a white phase under backscatter imaging) forms a fully sintered, well-connected aggregate network that extends from the 430 surface on the right to the LCM surface on the left. In comparison with the cross-sectional image of a 430SS/G-18 glass/430SS sandwich joining sample Fig. 5(b), processed under the same heat treatment conditions, it is also apparent that the microstructures of the two glasses are significantly different. The glassy material in Fig. 5(b) is partially devitrified and the resulting glass-ceramic composite and adjacent interface are composed of five microstructurally distinct zones: (a) the devitrified glass-ceramic 20+ μm away from the interface with the metal, (b) an adjacent glass-ceramic region that is measurably depleted in barium, (c) a ~10 μm thick reaction zone between the chromia scale and the glass, (d) a chromia scale that forms on the surface of the alloy during joining, and (e) the bulk 430 stainless steel. The devitrified glass is composed of several crystalline phases, notably: $BaSiO_3$ (oblate white crystals), $BaAl_2Si_2O_8$ (needle-shaped dark gray crystals), and $Ba_3CaSi_2O_8$ (large, blocky gray crystals), with the matrix composed of 11.6 mol% Si, 8.1 mol% Ba, 7.5 mol% Ca, 3.2 mol% Al, and 69.6 mol% O.

The matrix in the Ag-glass composite in Fig. 5(a) is not as uniform across the thickness of the joint as the devitrified glass in Fig. 5(b). Near the 430 interface, a thinner ~3-5 μm layer of barium chromate forms over the thin chromia scale. Further into the joint, there is a fairly wide band in the matrix that is primarily composed of barium calcium silicate sparsely populated by equiaxed barium silicate crystals. Mirroring this band on the opposite side of the joint adjacent to the LCM substrate is a thicker 40-50 μm band of the barium calcium aluminosilicate glassy matrix. Concentrated near the center of the joint and surrounding the Ag are coarse ~10 μm long $BaAl_2Si_2O_8$ needles embedded in a thin barium calcium silicate matrix.

The evolution of the interfaces within the conductivity samples as a function of time at temperature and current is shown in the two series of micrographs in Fig. 6 (430/Ag-glass interface) and Fig. 7 (Ag-glass/LCM interface). It is immediately obvious from all six micrographs that the interconnected Ag network does not coarsen or change significantly in morphology with time. However, the sequence of micrographs in Fig. 6 does show that the Ag begins to penetrate into the chromia scale during high temperature electrical testing, eventually forming a fairly extensive, nearly chromia-free Ag layer directly on the 430 surface after 750 h The reason for the diffusion of Ag toward the metal/composite interface is not known, although Ag electromigration or vaporization may play a key role. The migration of Ag through the semiconductive chromia scale may be one reason why the conductances of the double joint samples shown in Fig. 4 improve with time. The second significant microstructural change that is found in Fig. 6 is the diffusion of chromium into the glass matrix, which extends the barium chromate reaction zone further into the joint.

On the LCM side of the joint, Fig. 7(a)-7(c), the microstructure does not appear to change significantly with time at constant temperature and under constant current. EDX results indicate, however, that a ~1 μm thin reaction zone forms between the glass matrix and the LCM that is rich in lanthanum, manganese, calcium, silicon, and oxygen and contains 2-3 at.% barium. This zone appears to grow slightly thicker after 250 h at temperature and, by 750 h, has diffused into the LCM, forming individual reaction zones of the same composition within the porosity around each grain in the ceramic

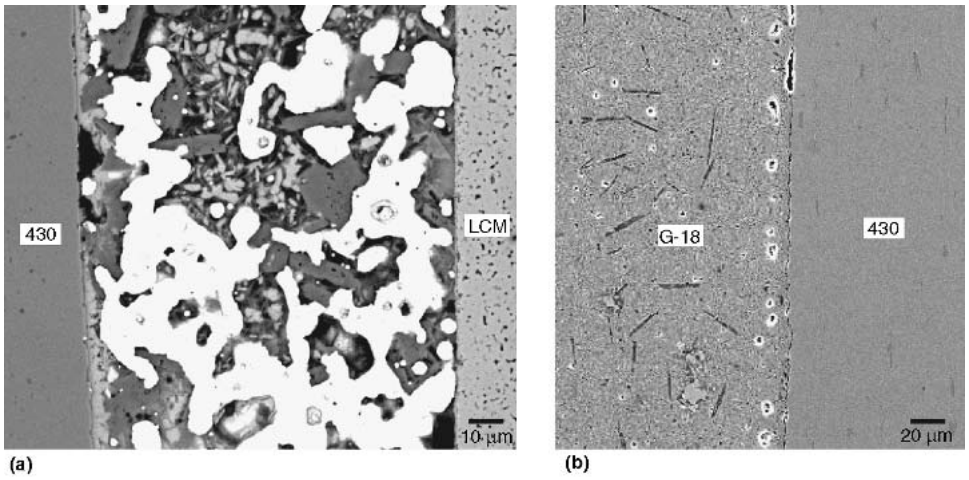


**Fig. 5** Cross-sectional SEM micrographs of **(a)** an as-formed LCM/ 35 vol% Ag-glass/430 joint and **(b)** a G-18 glass/430 half-joint

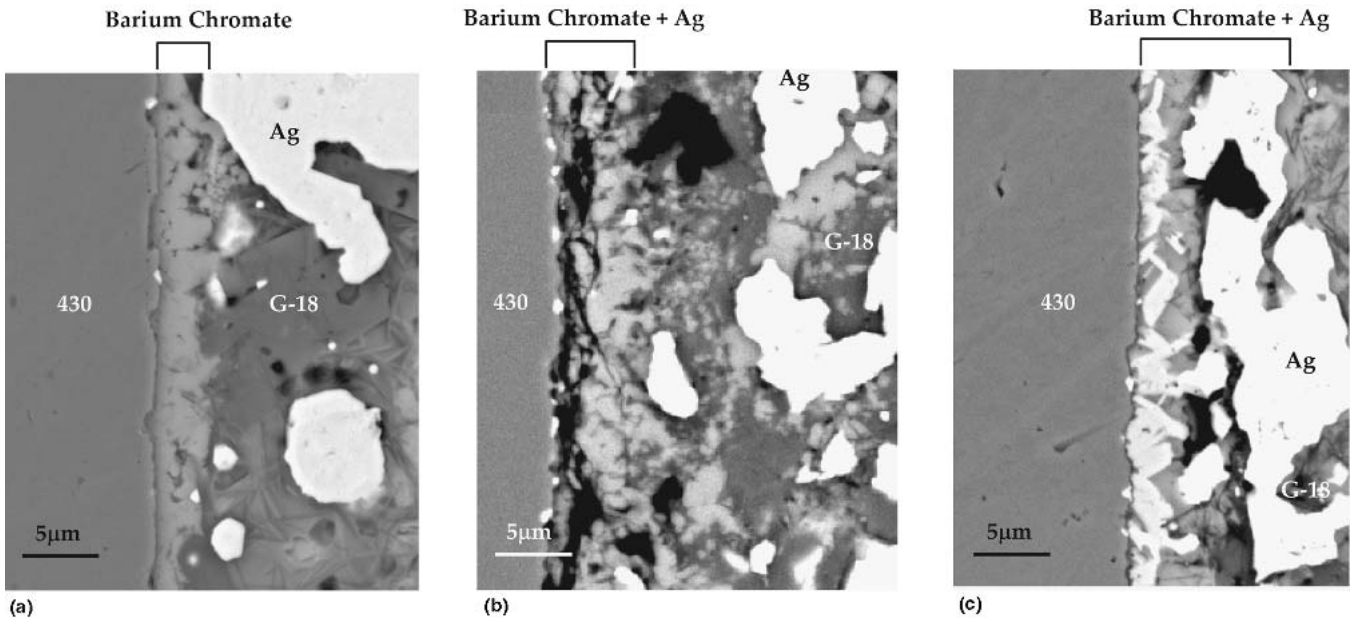


**Fig. 6** Cross-sectional SEM micrographs of the metal/glass-composite region in three LCM/ 35 vol% Ag-glass/430 joints which have been tested as follows: **(a)** as-formed, no testing, **(b)** 250 h at 750 °C, 1.5 A dc current, and 20 $cm^3$/min of dry air; and **(c)** 750 h at 750 °C, 1.5 A dc current, and 20 $cm^3$/min of dry air. Materials and phases in the joints are labeled.

substrate. On the other hand, the composition of the glass matrix away from the composite/LCM interface remains essentially unchanged.

## 4. Summary and Conclusions

MIECs have tremendous potential for use in a number of advanced commercial products, including chemical sensors, gas-separation devices, and solid oxide fuel cells. One of the major hurdles yet to be overcome with regard to these materials is to develop an appropriate means of joining them to the heat resistant interconnects used to transport electrical current to or from the MIEC and respective device. The key performance issues are: (a) the MIEC/metal interconnect joint must be structurally sound and (b) electrically conductive over thousands of hours at nominally 750 °C under a fairly high current density, on the order of 1.4 A/$cm^2$. There are a number of possible joining techniques that can be considered, the most promising of which appear to be those that use a composite joining material.

One such material, a Ag-glass composite was examined in detail and shown to display good wetting and spreading properties on $(La_{0.8}Ca_{0.2})MnO_3$ and 430 stainless steel substrates. In addition, the room temperature, through-thickness resistances of these half-joints were quite low indicating that the

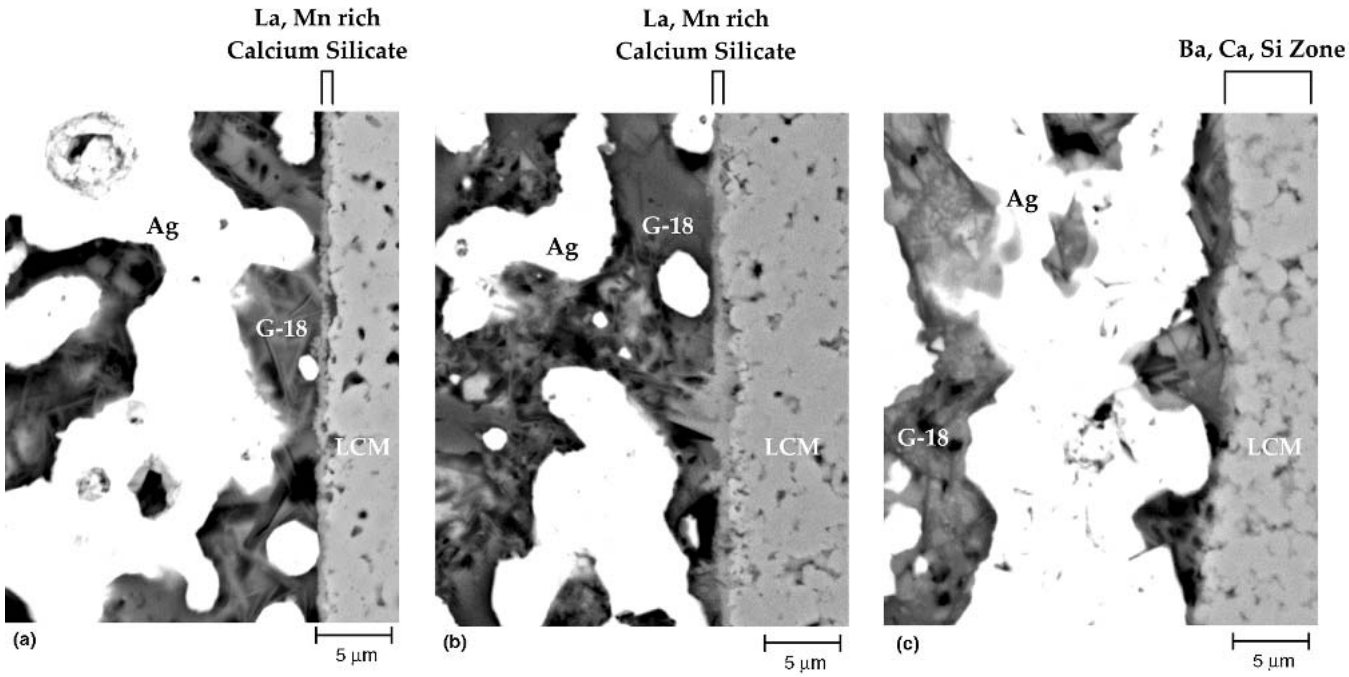


**Fig. 7** Cross-sectional SEM micrographs of the metal/glass-composite region in three LCM/ 35 vol% Ag-glass/430 joints which have been tested as follows: **(a)** as-formed, no testing, **(b)** 250 h at 750 °C, 1.5 A dc current, and 20 $cm^3$/min dry air; and **(c)** 750 h at 750 °C, 1.5 A dc current, and 20 $cm^3$/min of dry air. Materials and phases in the joints are labeled.

current path through the bulk composite and the composite/substrate interfaces were relatively free of non-conductive reaction layers. 250 and 750 h electrical testing of LCM/35 vol% Ag-glass/430 joints at 750 °C demonstrated no degradation in the electrical conductances of these joints. In fact, the conductance appeared to improve slightly with time. Metallographic and EDX results suggest that the improved performance may be due to penetration of the semiconductive chromia scale that forms on the metal during joint processing by highly conductive Ag from the adjacent composite.

## Acknowledgments

The author would like to thank Nat Saenz, Shelly Carlson, and Jim Coleman for their assistance in metallographic and SEM sample preparation and analysis and Dong Kim and Kerry Meinhardt for helpful discussions about the glass matrix and assistance in preparing the tape cast LCM samples. This work was supported by the U. S. Department of Energy, Office of Fossil Energy, Advanced Research and Technology Development Program. The Pacific Northwest National Laboratory is operated by Battelle Memorial Institute for the United States Department of Energy (U.S. DOE) under Contract DE-AC06-76RLO 1830.

## References

1. G.R. Doughty and H. Hind: "The Applications of Ion-Conducting Ceramics," *Key Eng. Mater.*, 1996, *122-24*, pp. 145-62.
2. H. Meixner and U. Lampe: "Metal Oxide Sensors," *Sens. Actuators B*, 1996, *33*, pp. 198-202.
3. N.Q. Minh: "Ceramic Fuel Cells," *J. Am. Ceram. Soc.*, 1993, *76*, pp. 563-88.
4. A.V. Kovalesky, V.V. Kharton, V.N. Tikhonovich, E.N. Naumovich, A.A. Tonoyan, O.P. Reut, and L.S. Boginsky: "Oxygen Permeation Through $Sr(Ln)CoO_{3-\delta}$(Ln = La,Nd,Sm,Gd) Ceramic Membranes," *Mater. Sci. Eng. B*, 1998, *52*, pp. 105-16.
5. A.J. Appleby: "Fuel Cell Technology: Status and Future Prospects," *Energy*, 1996, *21*, pp. 521-653.
6. B. Ma, U. Balachandran, J-H. Park, and C.U. Segre: "Electrical Transport Properties and Defect Structure of $SrFeCo_{0.5}O_x$," *J. Electrochem. Soc.*, 1996, *143*, pp. 1736-44.
7. S.P. Simner, K.D. Meinhardt, and J.W. Stevenson, Pacific Northwest National Laboratory, 902 Battelle Blvd., P.O. Box 999, Richland, WA 99352, private communication.
8. R.G. Loasby, N. Davey, and H. Barlow: "Enhanced Property Thick-Film Conductor Pastes," *Solid State Technol.*, 1972, *15*, pp. 46-50.
9. N.S. Witte, P. Goodman, F.J. Lincoln, R.H. March, and S.J. Kennedy: "Electrical and Magnetic Phases of the Layered Perovskite $Ca_{4-x}La_xMn_3O_{10}$," *Appl. Phys. Lett.*, 1998, *72*, pp. 853-55.
10. K. Huang, J. Wan, and J. B. Goodenough: "Oxide-Ion Conducting Ceramics for Solid Oxide Fuel Cells," *J. Mater. Sci.*, 2001, *36*, pp. 1093-98.
11. R. Mahesh and M. Itoh, Mitsuru: "Effect of Oxygen Stoichiometry on the Structure, Magnetism and Electron Transport Properties of the Rare Earth Manganates Exhibiting Charge Ordering," *Sol. St. Ionics*, 1998, *108*, pp. 201-08.
12. K.D. Meinhardt, J.D. Vienna, T.R. Armstrong, and L.R. Pederson: U. S. Patent No. 6 430 966, 2002.
13. K.S. Weil, J.E. Deibler, J.S. Hardy, D.S. Kim, G-G. Xia, L.A. Chick, and C.A. Coyle: "Rupture Testing as a Tool for Developing Planar Solid Oxide Fuel Cell Seals," *J. Mater. Eng. Perf.*, 2004, *13*(3), pp. 316-26.
14. B.E. Springett: "Conductivity of a System of Metallic Particles Dispersed in an Insulating Medium," *J. Appl. Phys.*, 1973, *44*, pp. 2925-26.